Experimental and Simulation Study on CO2 Adsorption Dynamics of a Zeolite 13X Column during Blowdown and Pressurisation: Implications of Scale-up on CO2 Capture Vacuum Swing Adsorption Cycle

Experimental and Simulation Study on CO_2 Adsorption Dynamics of a Zeolite 13X Column during Blowdown and Pressurisation: Implications of Scale-up on CO_2 Capture Vacuum Swing Adsorption Cycle

Hyungwoong Ahn[1)]*, Suk-Hoon Hong[2)], Yixuan Zhang[1)], Chang-Ha Lee[2)]

1) Institute for Materials and Processes, School of Engineering, The University of Edinburgh, Robert Stevenson Road, Edinburgh EH9 3FB, UK

2) Department of Chemical and Biomolecular Engineering, Yonsei University, 50 Yonsei-ro, Seodaemun-Gu, Seoul, 03722, Republic of Korea

*Corresponding author. Tel.: +44 131 650 5891

E-mail address: H.Ahn@ed.ac.uk

Abstract

A 13X column Vacuum Swing Adsorption (VSA) has been widely studied as a promising separation process for post-combustion carbon capture, as it has been claimed that it would be more economical than conventional amine capture processes. To advance its commercial application, however, it is crucial to have a VSA achieve an excellent bed productivity, well beyond the current level, to enable the process to work

for a larger CO_2 emission plant in an affordable size. From the perspective of adsorption process design, its bed productivity could be improved by reducing the adsorption cycle time. In other words, the pressure change between adsorption and desorption steps must take place as quickly as possible. In this study, CO_2 adsorption dynamics of a 13X column during the pressure-changing steps, i.e. blowdown and pressurisation, were investigated by both experiments and numerical simulation. As a result, it turns out that the blowdown time must be extended greatly with increasing column length due to the pressure change being hindered by the pressure drop building up inside the column. In the stark contrast, the pressurisation time is rarely affected by the column length but it can be controlled easily by the rate of changing the pressure on one column end. This result implies that the bed productivity would be compromised greatly in scaling up a 13X VSA, due to the cycle time having to be extended long enough to accommodate the stretched blowdown time. To address this scale-up issue, an adsorption column design technology, stacking low-height, packed-bed adsorption modules vertically, was proposed. The new adsorption column design paved the way for enabling a 13X VSA to achieve as high a productivity as its lab-scale unit, no matter which size it is to be scaled up to, without having to adjust the bead size.

Keywords: CO_2 capture; 13X; Blowdown; Pressurisation; Scale-up; Productivity

1. Introduction

The Climate Change Act 2008 made the UK the first country to introduce a long-term, legally-binding national legislation to tackle climate change, putting forward a target to reduce its Greenhouse Gas (GHG) emission up to 80% of 1990 levels in 2050. Around 10 years after the climate change act became law, the Committee on Climate Change

(CCC) revised the 2050 target in 2019 so that the UK aims to reduce the GHG emissions by at least 100% of 1990 levels, in other words, net zero emission [1]. CCC declared that to achieve this highly challenging target it is essential to decarbonise the power and industrial plants running on fossil fuels by CCS (Carbon Capture and Storage). Negative emission through DAC (Direct Air Capture) and BECCS as well as fossil CCS would make it easier to achieve the revised 2050 GHG emission target. Up to now, more attention has been paid to CO_2 capture from large, point sources, e.g. fossil-fuel power plants and industrial plants (cement, chemical, steel/iron, etc.), than small- to medium- scale, distributed sources. To meet the stringent 2050 target, however, it is crucial to decarbonise power and industrial plants running on fossil fuels no matter which size of the plant it is.

As of 2019, a commercial CCS plant has not been constructed in the UK yet, which is mainly attributed to unsatisfactory economic feasibility rather than technical issues [2]. For a large-scale application, absorption processes using physical or chemical solvents are likely to be most reliable and economical for pre- or post- combustion capture, respectively. However, it was estimated that the cost of electricity would increase up to double the current level, when a fossil fuel power plant was to be decarbonised by CCS [3].

An amine capture plant, the most conventional post-combustion capture process, involves both huge capital and operating costs. In particular, the energy consumption amounting to 1.38 MJ_e/kg CO_2 could be mitigated by process intensifications enabling more efficient use of the energy supplied, but the reduction of the energy consumption through process intensification was estimated only 14% at the most [4]. In case of a SMR H_2 plant integrated with the amine capture plant, both the capital cost and the fuel cost would increase substantially to double those of the non-capture plant [5]. As an

alternative to the energy-intensive absorption process, solid adsorption has a good potential to bring down the capture cost by half [6, 7]. Now that it is crucial to implement CCS on the plants emitting CO_2 of any scale to meet the new 2050 target, it is important to develop further every emerging capture technology, including adsorption, having in mind that in general adsorption would be more suitable for gas separation at small- to medium- scale plants than large-scale plants [8].

The most notable downside of adsorption processes is that they are often difficult to scale up. For oxygen production from air, for example, adsorption has been known to be superior to absorption/distillation for small-scale applications, e.g. medical oxygen production. But cryogenic distillation is more advantageous than adsorption for large-scale applications, e.g. oxygen production for an IGCC power plant [8, 9]. However, the intrinsic poor scalability issue of an adsorptive capture process could be alleviated to some extent by reducing the cycle time leading to enhancing the process productivity defined as CO_2 production rate per column volume or adsorbent mass.

Zeolite 13X is a commercial synthetic adsorbent owning an excellent adsorption capacity of CO_2 even in its very low concentration range and it also has a decent selectivity of CO_2 over N_2 [10]. Hence, a number of adsorptive carbon capture processes have been designed with zeolite 13X [7, 11-22], and the zeolite 13X process was taken as a reference case for evaluating new adsorptive capture processes designed with emerging porous materials [10, 23]. In the past works, however, they designed, simulated or experimented various CO_2 capture adsorption processes at lab scales, with the column lengths ranging 0.2 to 1.0 meter at most, not addressing what would happen to the designed process when it was scaled up for commercialisation.

To facilitate handling of the adsorbents, 13X crystals are pelletized into beads of various sizes. It has been found that macropore diffusion would be a rate-controlling

step in the course of CO_2 diffusing into 13X beads characterised by bi-disperse pore structure [24]. Therefore, it would be advantageous to make use of 13X beads of small size for the adsorption column, in order to have the adsorption system have a short diffusion time constant, or reducing diffusive effects, so that it can be more equilibrium-driven process with the process performance improved.

However, reducing the bead size involves inevitably greater pressure drops along the column, to an extent of limiting the feed flowrate an adsorption process can process. The pressure drop along the packed bed occurring due to the friction exerting on a fluid flowing through porous media may become more conspicuous in pressure-varying steps than pressure-constant steps, in case the pressure change is forced to occur very fast to reduce the cycle time. Abrupt change of pressure causes an extremely high flowrate of the gas passing through the column, which may lead to considerable pressure drop along the column. In other words, the pressures at the two ends of a column change differently during the pressure-varying steps, i.e. the pressure at the closed end trailing the pressure at the open end through which the gas enters or leaves the column. In order to get the trailing pressure to reach the target pressure, the gas velocity must decrease so low that the pressure drop becomes negligible. Strictly speaking, it is not until the pressure drop goes to null that a pressure change step is finished.

In this study, the dynamics of a 13X column undergoing blowdown or pressurisation are to be studied by both experiments and simulations. The blowdown experiments were performed with the column initially saturated with CO_2, to mimic the column dynamics in the blowdown step of a heavy-reflux VSA cycle. It was reported that the heavy reflux step in which a column is swept by a pure CO_2 stream prior to blowdown could make it easier to achieve high CO_2 purity [22, 25]. To see the effect of adsorption capacity on

column dynamics during the pressure-varying steps, the experiments were repeated with Helium in place of CO_2.

2. Blowdown and Pressurization Experiments

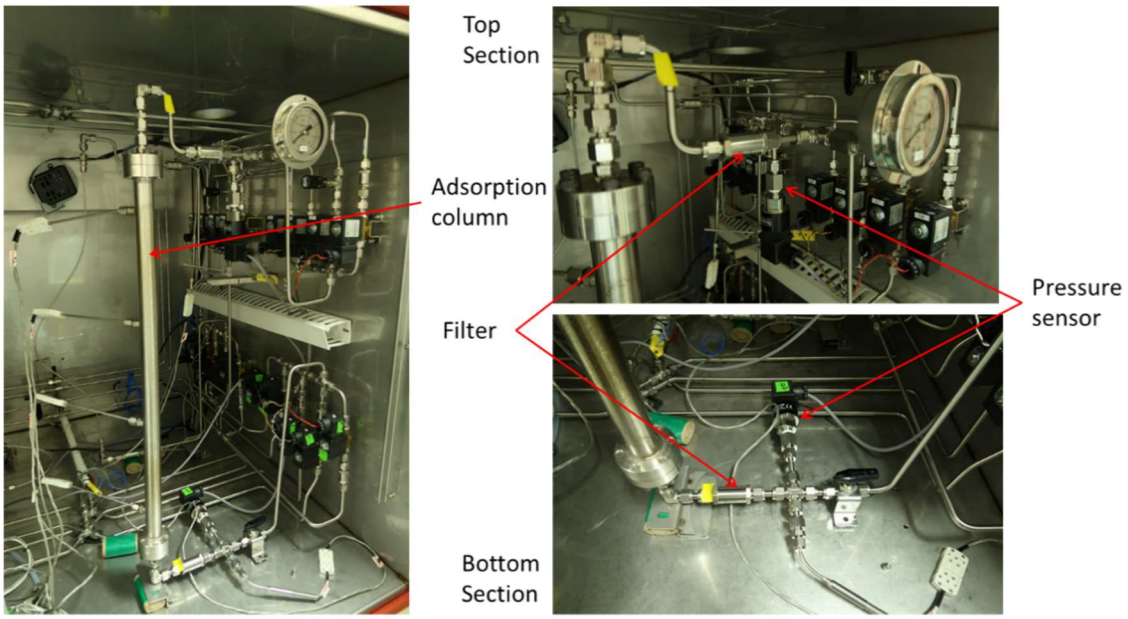

Figure 1. Photos of the experimental apparatus for blowdown and pressurisation experiments.

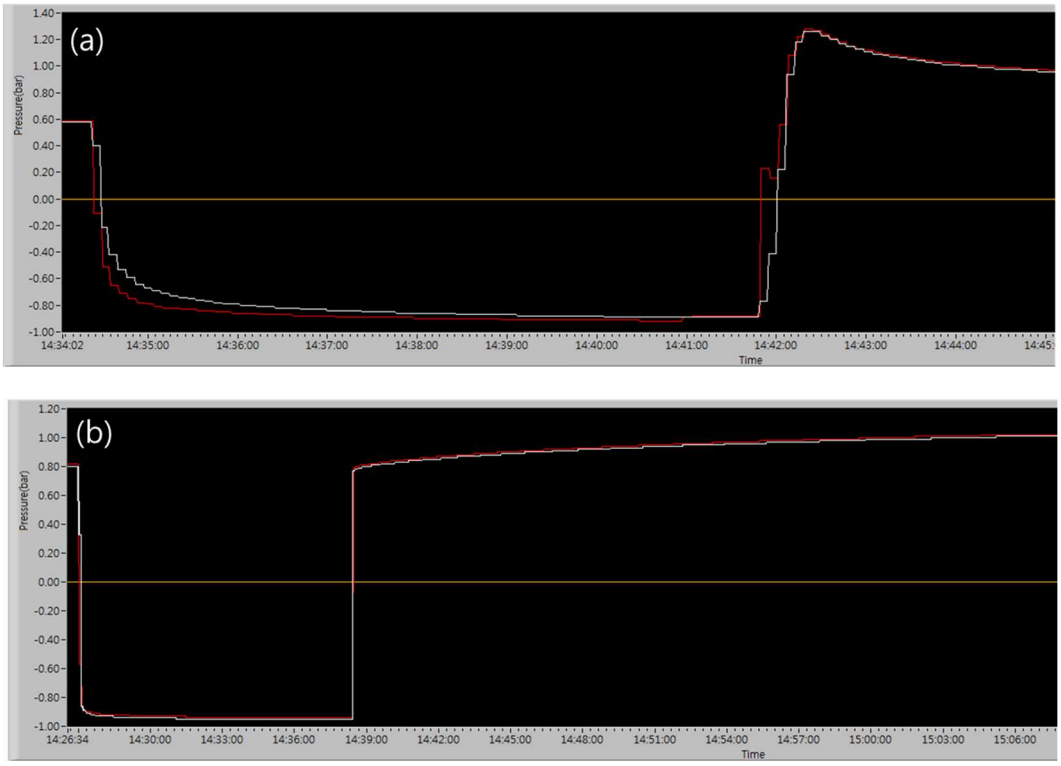

Figure 2. Pressure profiles measured at the top and bottom sections in the blowdown experiment followed by pressurisation experiment: (a) CO_2 and (b) He.

A lab-scale pressure swing adsorption rig was employed for blowdown and pressurisation experiments. The adsorption column was placed inside an oven as shown in Figure 1. The dimension and properties of the adsorption column are listed in Table 1. The adsorbents chosen in this study were UOP Molsiv 13X APG (4×8 Beads). The adsorption column was densely packed with thermally activated 13X beads with the column tapped constantly throughout the loading. The beads inside the column were held tightly by glass wools and meshes placed on both column ends. Once the packed column was inserted into the adsorption system, it was regenerated again in situ by heating the system at 180 °C by the oven's electric heater in vacuum condition for 6 hours. Once the column was cooled, it was pressurised with CO_2 (or He) up to 0.6 – 0.8 barg (see Figure 2). When the column pressure and temperature were stabilised, the blowdown experiment commenced by pulling a vacuum through the column bottom. The column was depressurised up to around –0.9 barg. In the blowdown run, the column was evacuated by opening the valve connecting to a vacuum pump (DA-60D, ULVAC, Japan) in the bottom section with the valve in the top section closed. As seen in Figure 1, an in-line filter (SS-4F-7, Swagelok, US) was placed on the top and bottom sections of the column, to protect the instruments installed on the lines, e.g. pressure sensors, from fragments and dusts that may be generated off the column by contact between fluids and adsorbent beads. The pressure drop through the filter turned out to be significant in the pressure-varying processes and its contribution to the overall pressure drop will be discussed in details later on. During the experiments the column pressure changing with time was monitored by pressure transducers (PSC, Sensor System Technology, Korea) placed in the top and bottom sections (see Figures 1 and 2). It should be noted that the position at which the sensor measures the pressure is not at the column end but downstream (blowdown) or upstream (pressurisation) of the filter. Therefore, the pressure measured in the bottom section must include the effect of

pressure drop through the filter of which the contribution to the overall pressure drop is often not negligible. The blowdown run proceeded until the pressure on the closed end reached the target pressure. Once the pressure and temperature were stabilised, the pressurisation run commenced by feeding CO_2 (or He) through the bottom section with the valve on the top still closed. In the pressurisation runs, therefore, the gas travelled in the opposite direction to the gas flow in the blowdown runs. The target pressure to reach at the end of the pressurisation run is controlled by a back pressure regulator (P-702C-FA-22-V, Bronkhorst High-Tech, NL) installed on the top section.

3. Mathematical model for adsorption column in pressure-varying steps

To simulate the pressure-varying processes of an adsorption column, a set of mathematical equations of mass, energy and momentum balances around the adsorption column need to be solved simultaneously. Below are the mathematical models taken for full numerical simulation of this study.

For a fixed column which an adsorptive pure component flows through, its mass balance equation is constructed by:

$$\frac{\partial c_T}{\partial t} + \frac{\partial (u \cdot c_T)}{\partial z} + \frac{1-\varepsilon}{\varepsilon} \rho_b \frac{\partial \overline{q}_i}{\partial t} = 0 \qquad (1)$$

Linear Driving Force (LDF) model was taken to estimate the adsorption rate.

$$\frac{\partial \overline{q}_i}{\partial t} = k_{LDF,i} \cdot (q_i^* - \overline{q}_i) \qquad (2)$$

in which the LDF coefficient is estimated by:

$$k_{LDF,i} = \frac{c_i}{q_i \rho_s} \frac{15 \varepsilon_p D_p}{r_p^2} \tag{3}$$

For a pure component system, pore diffusivity, D_p, is a combination of the Knudsen and viscous diffusivity as follows:

$$D_P = \frac{D_K + D_v}{\tau} \tag{4}$$

Knudsen and viscous diffusivity are estimated by:

$$D_K = \frac{2}{3} r \sqrt{\frac{8\Re T}{\pi M}},\ D_v = \frac{Pr^2}{8\mu} \tag{5}$$

As can be seen in Eq.(3), the LDF coefficient for CO_2 adsorption in the pelletized zeolite 13X was estimated by macropore diffusivity [13], given the finding that the overall diffusion rate is dominated by diffusion in the macropore [24].

Assuming instantaneous thermal equilibrium between the mobile and stationary phases, the energy balance equation is given by [26]:

$$\begin{aligned} &\left(\hat{C}_{vg} \rho_g + \frac{1-\varepsilon}{\varepsilon} \cdot \hat{C}_{ps} \rho_s + \frac{1-\varepsilon}{\varepsilon} \cdot \hat{C}_{pa} \rho_{ads} \right) \frac{\partial T}{\partial t} - k_z \frac{\partial^2 T}{\partial z^2} \\ &+ \hat{C}_{vg} \rho_g u \cdot \frac{\partial T}{\partial z} - \frac{1-\varepsilon}{\varepsilon} \cdot \sum_{i=1}^{n} \left(-\Delta H_i - RT \right) \frac{\partial \overline{q}_i}{\partial t} + \frac{\partial uP}{\partial z} + \frac{2h_{in}}{\varepsilon R_{in}} \left(T - T_w \right) = 0 \end{aligned} \tag{6}$$

As the column is not adiabatic, the heat balance around the wall was constructed as follows:

$$\left(\hat{C}_{pw} \rho_w \right) \frac{\partial T_w}{\partial t} - k_w \frac{\partial^2 T}{\partial z^2} - 2R_{in} h_{in} \frac{T - T_w}{R_{out}^2 - R_{in}^2} + 2R_{out} h_{out} \frac{T_w - T_a}{R_o^2 - R_i^2} = 0 \tag{7}$$

As for the momentum balance, Ergun equation was chosen to estimate the pressure drop along the column length.

$$-\frac{dP}{dz}=\frac{150\cdot\mu\cdot u\cdot(1-\varepsilon)^2}{d_P^2\cdot\varepsilon^2}+\frac{1.75\cdot(1-\varepsilon)\cdot\rho_g\cdot u\cdot|u|}{d_P\cdot\varepsilon} \quad (8)$$

A dual-site Langmuir isotherm was taken for estimating the equilibrium adsorption amount of CO_2 on zeolite 13X [27].

$$q_i^{eq}=\frac{q_{sb,i}b_ic_i}{1+\sum_i b_ic_i}+\frac{q_{sf,i}f_ic_i}{1+\sum_i f_ic_i} \quad (9)$$

where b_i and f_i are a function of temperature.

$$b_i=b_{i,0}e^{\frac{-\Delta U_{b,i}}{RT}} \quad (10)$$

$$f_i=f_{i,0}e^{\frac{-\Delta U_{f,i}}{RT}} \quad (11)$$

Given the chosen adsorption isotherm, the heat of adsorption must vary with temperature and pressure. At 298K, the heat of adsorption decreases with pressure, starting from 39103 J/mol at 0 kPa and converging to 38194 J/mol with increasing pressure. At 50 kPa, it increases with temperature from 38201 J/mol at 270 K to 38557 J/mol at 330 K. In this study, a constant value of 38300 J/mol was taken as the heat of adsorption averaged over the operating conditions.

The axial thermal dispersion coefficient, k_z, was estimated using the correlation proposed by Wakao and Funazkri [28]:

$$\frac{k_z}{k_g}=7+0.5\cdot\mathrm{Pr}\cdot\mathrm{Re} \quad (12)$$

Danckwert boundary conditions were taken for estimating the gas concentration and enthalpy at both column ends [18]. The DAEs listed above were solved by PSE gPROMS with the second-order orthogonal collocation on finite elements (OCFEM). The simulation parameters are listed in Table 1.

In simulating a pressure-varying step, it is important to find an equation capable of fitting best the pressure change at the column end through which a gas flows from the initial to the final state. And the speed and trajectory of the column end pressure changing with time can be affected by various factors, such as sizes of pipe and valve, feed supply pressure (pressurisation) or vacuum pump capacity (blowdown), etc. It is always desirable to make the column end pressure reach the target pressure as quickly as possible in case of a rapid pressure swing cycle aiming for maximising the bed productivity.

In this study, the experimental pressure profile at the column end adjacent to the valve through which a gas flows was fitted by one of the following two equations:

$$P(t)=(P_H-P_L)e^{-\alpha t}+P_L \quad \text{Blowdown} \qquad P(t)=(P_L-P_H)e^{-\alpha t}+P_H \quad \text{Pressurisation} \qquad (13)$$

$$P(t)=\frac{P_H-P_L}{\alpha t(P_H-P_L)+1}+P_L \quad \text{Blowdown} \qquad P(t)=\frac{-P_H+P_L}{\alpha t(P_H-P_L)+1}+P_H \quad \text{Pressurisation} \qquad (14)$$

in which the α was found such that simulated pressures in the bottom section can match best the experimental pressure data.

Table 1. Physical properties and adsorption parameters of the zeolite 13X bead and the adsorption column.

Column parameters	
Column length [m]	0.55
Column inner diameter [m]	0.0225
Column outer diameter [m]	0.0255
Interparticle void fraction, ε [-]	0.2576
Bed density [kg/m^3]	780
Wall density, ρ_w [kg/m^3]	7800
Specific heat capacity of the wall, C_{pw} [J/kg·K]	502
Inner heat transfer coefficient at the wall, h_i [W/m^2·K]	10
Outer heat transfer coefficient at the wall, h_o [W/m^2·K]	3

Gas and adsorbed phase parameters	
Axial mass dispersion coefficient, D_z [m^2/s]	$1.0\ 10^{-3}$
Axial thermal dispersion coefficient, k_z [W/m·K]	$1.6\ 10^{-3}$
Specific heat capacity of the gas, C_{pg} [J/kg/K]	844
Specific heat capacity of the adsorbed phase, C_{pa} [J/kg·K]	1344
Gas viscosity at 1 bar, 25 C, μ [Pa s]	$1.46\ 10^{-5}$ (CO_2) / $1.96\ 10^{-5}$ (He)
Zeolite 13X (UOP APG Molsiv) parameters[29, 30]	
Particle density, ρ_s [kg/m^3]	1050
Skeletal density, [kg/m^3]	2300
Macropore porosity. [-]	0.292
Average macropore diameter, [nm]	281.3
Specific heat capacity, C_{ps} [J/kg/K]	920
Particle diameter, d_p [mm]	2.01
Dual-site Langmuir Isotherm Parameters (CO_2)[13]	
q_{sb} [mol/kg]	3.09
q_{sf} [mol/kg]	2.54
b_0 [m^3/mol]	$8.65\ 10^{-7}$
f_0 [m^3/mol]	$2.63\ 10^{-8}$
$-\Delta U_b$ [J/mol]	36641.21
$-\Delta U_f$ [J/mol]	35690.7

4. Results and discussion

4.1. Blowdown cases

As shown in Figure 2(a), it is certain that two pressure profiles in the top and bottom sections exhibited visible discrepancy during the CO_2 blowdown and pressurisation, indicating that there existed a considerable pressure drop along the path between the two positions. Several items were considered flow resistances that might account for the pressure drop: glass wools/meshes on the column ends, unions and filters on the tube, as well as packed bed itself. In this case, it was reasonably assumed that the observed pressure drop would be ascribed to two frictional losses through the packed column and the filter that are relatively salient with the others small enough to neglect.

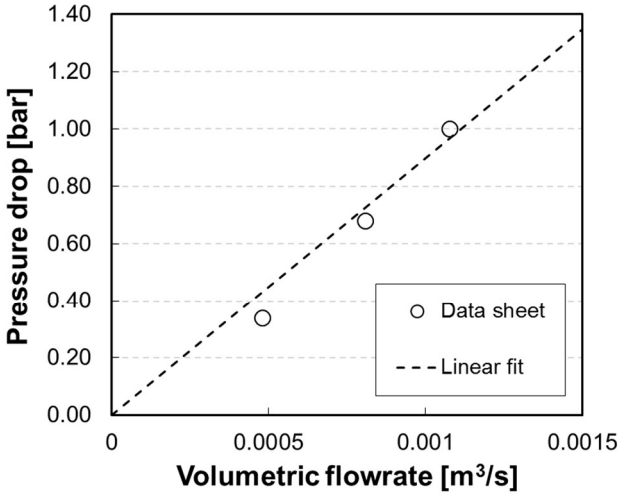

Figure 3. Relation of pressure drop across the filter with gas flowrate [31].

To estimate the pressure drop through the filter, it is necessary to see how large the inlet pressure has to be so as to make a gas flow through the filter at a certain fluid flowrate, i.e. relationship between gas flowrate and pressure drop, in the range of gas flowrates encompassing the experimental conditions. As for the relationship, a Swagelok brochure on the specific filter used in this study provided useful information of flow data in which air flowrates through the filter up to 0.001076 m^3/s were measured at different inlet pressures with the discharge pressures all identical at ambient pressure [31]. To make it easier to find the pressure drop at a given gas flowrate, a linear equation fitting best the experimental data was found as below:

$$\Delta P[bar] = 900 F_v[m^3/s] \tag{15}$$

The experimental flowrate-pressure drop data reported in the brochure and the proposed correlation equation are plotted in Figure 3. In this study, the pressure drop through the filter was estimated by Eq. 15 from the gas flowrate obtained by numerical simulation. As the maximum interstitial velocity was around 9 m/s, the maximum gas flowrate in this simulation study was 0.0009218 m^3/s, lying within the range of the gas

flowrate tested by Swagelok for the correlation in Figure 3.

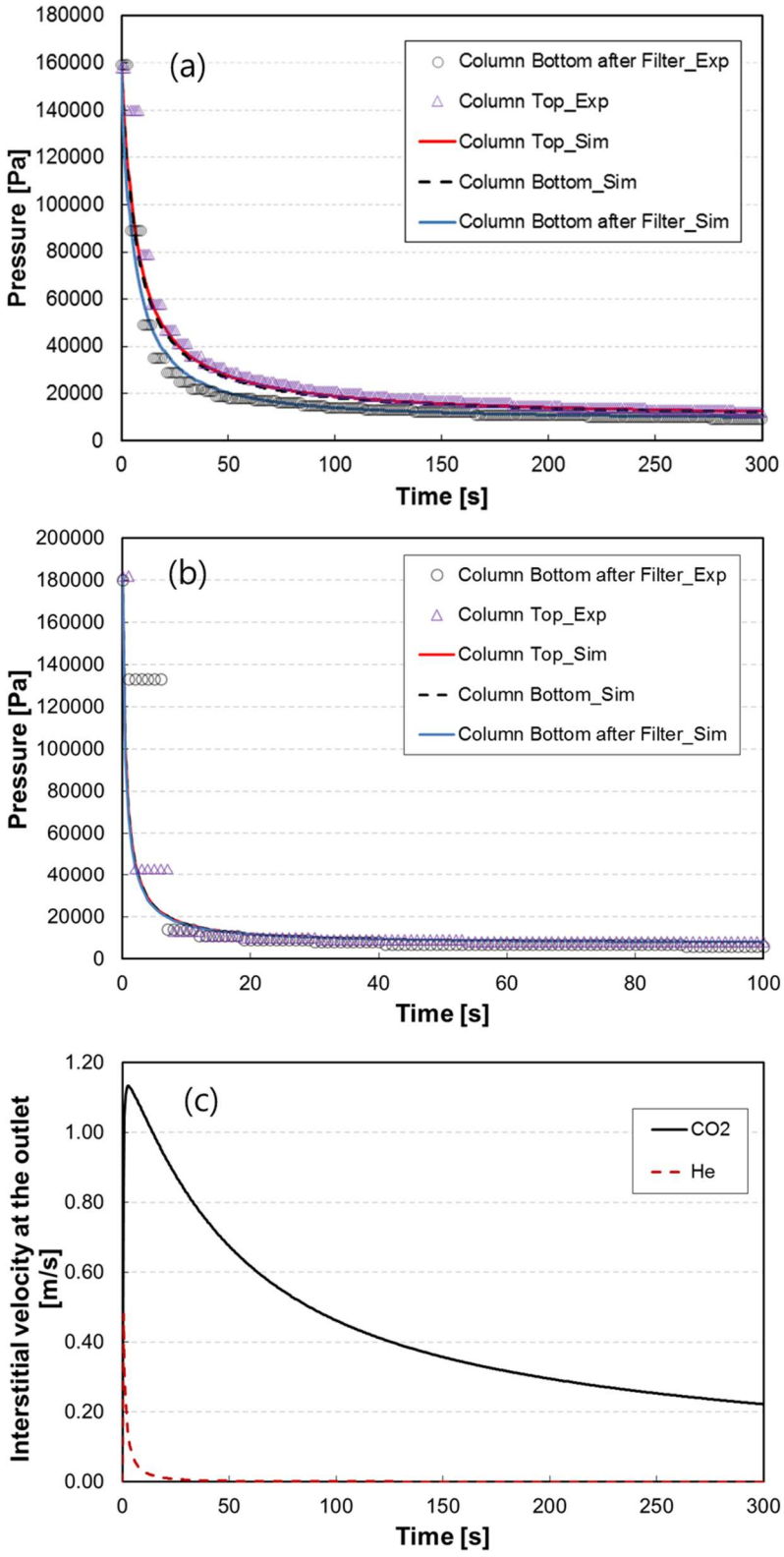

Figure 4. Pressure profiles of the adsorption column in blowdown runs in which the column was initially saturated with (a) CO_2 or (b) He. (c) Gas velocity profiles at the column exit in the blowdown runs.

Figure 4 shows blowdown dynamics of the adsorption column initially pressurised by either CO_2 or He in terms of the pressures at various positions and the gas velocity at the column exit. The symbols on Figure 4a and b are the experimental pressure data in Figure 2. In case of CO_2 (Figure 4a), the two experimental pressure profiles measured around the column (see Figure 1) show noticeable discrepancy, while they were practically identical in the He blowdown (Figure 4b). In the CO_2 blowdown run, the experimental pressure profiles indicate significant pressure drop existing over the path between the two measuring positions and it is needed how much each of the two steps causing pressure drop, i.e. packed column and filter, accounted for the overall pressure drop.

As seen in Figure 4c, the simulated gas velocity in the CO_2 blowdown run was much greater than the He velocity, mainly due to the huge adsorption amount of CO_2 compared to inert He, i.e. vast difference of the initial amount of the gas the column contained before evacuation. Now that the gas velocity was obtained by simulation, we could estimate the pressure drop associated with the filter in the bottom section by Eq. 15. The new pressure profiles including the pressure drop through the filter were added to Figures 4a and b. As shown in the feed pressure, the simulated pressure profile at the top end denoted by the red solid line was so close to the imposed pressure profile (Eq. 14) denoted by the black dashed line that the pressure drop along the column could not explain the noticeable difference of the experimental pressures measured at the two positions. Due to the high gas velocity of the CO_2 case, however, the pressure drop through the filter was estimated so huge that the simulated pressure profile in the bottom section denoted by the blue solid line in Figure 4a could match well the experimental pressure.

In jarring contrast to the CO_2 blowdown, the He blowdown run did not show a noticeable pressure drop in the experiment, nor in the simulation as shown in Figure 4b. This can be explained by huge difference of the gas flowrate through the system between the two cases. Due to such a low gas flowrate, the pressure drop through the filter as well as the column was negligible. And the time taken for depressurisation was highly affected by the pressure drop intensity.

The CO_2 and He blowdown are considered as two limiting cases, and an actual blowdown operation of a VSA will behave somewhere between the two limiting cases. In case of a cycle with a heavy-reflux step, the column is almost saturated with CO_2 after a heavy-reflux step, so its blowdown must be similar to the pure CO_2 case. Without a heavy-reflux step in a cycle, the column would be evacuated from an initial condition containing more N_2 and less CO_2. Accordingly, it would be easier to evacuate the column, so the blowdown would take less time than the pure CO_2 case but still needs more time than the pure He case.

4.2. Pressurisation cases

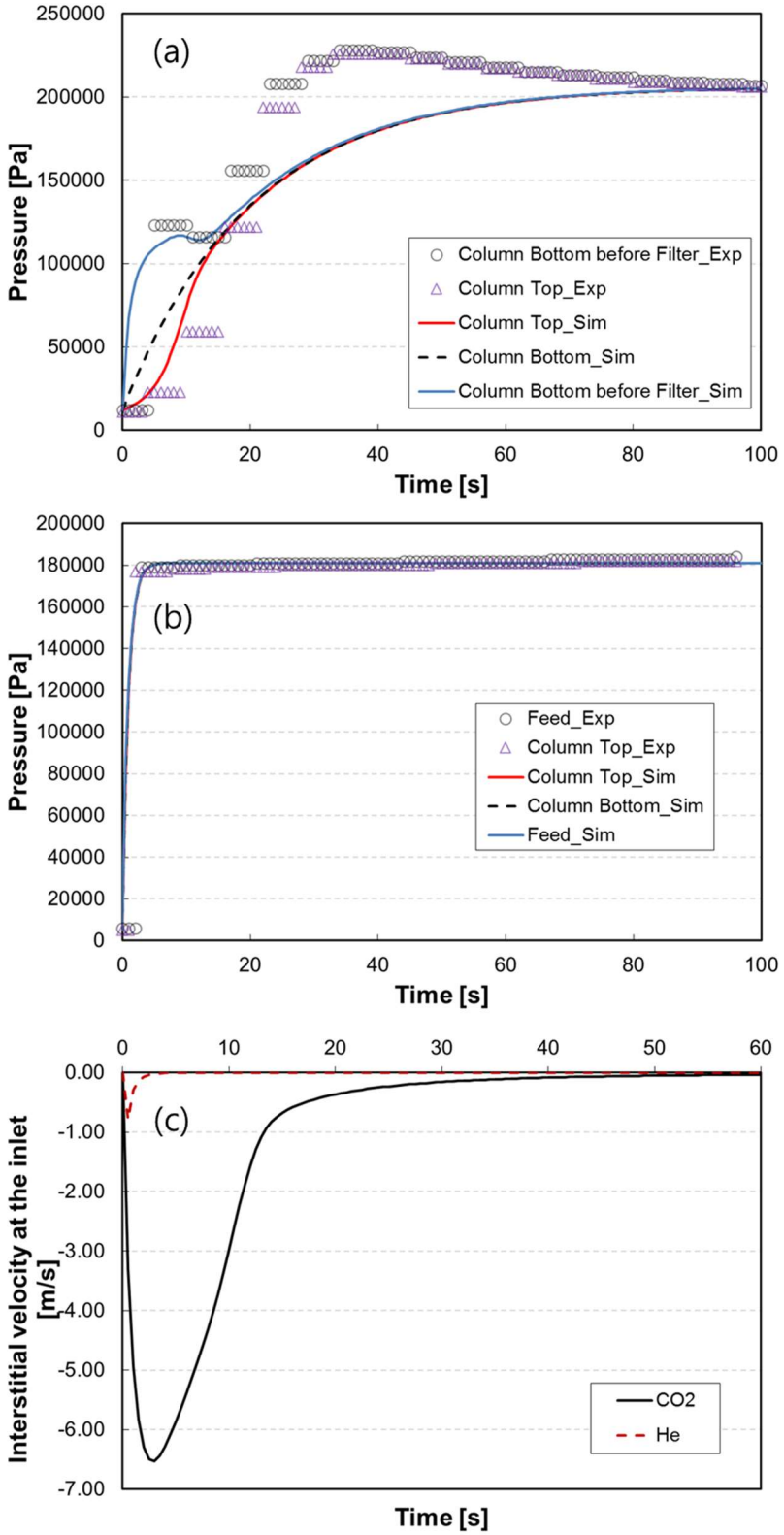

Figure 5. Pressure profiles of the adsorption column in pressurisation runs in which the column is pressurized with (a) CO_2 or (b) He. (c) Gas velocity profiles at the column inlet in the pressurisation runs.

The CO_2 pressurisation run also exhibited noticeable difference of the two pressure profiles in the top and bottom sections, but the column dynamics were very different from what were observed in the CO_2 blowdown run. As seen in Figure 5a, the experimental pressure readings at the two positions showed huge difference initially. However, the pressure difference lasted only for such a short time as the first 20 seconds or so, and then disappeared quickly. As a result, any pressure difference was not observed around 30 seconds after the onset of the experiment. Compared to the short but large pressure difference in the CO_2 pressurisation run, the CO_2 blowdown run showed the pressure difference was small in magnitude, but diminished gradually over so long a time as 300 seconds (see Figure 4a). It was of interest to see if the simulation was capable of predicting how the experimental pressure drop evolved during the run, i.e. the pressure drop that was large in magnitude but existed only for the first 20 seconds or so. The feed pressure measured upstream of the filter in the bottom section could not be obtained by simulation directly, but estimated indirectly by adding the pressure drop through the filter (Eq. 15) to the pressure at the bottom end of the column imposed by Eq. 13. As shown in Figure 5a, the simulated pressure profile in the bottom section (blue solid line) was in good agreement with the experimental data (circles), after the simulated pressure at the column bottom (black dashed line) was corrected for the pressure drop through the filter by Eq. 15. Again such a pressure difference was not observed in the He pressurisation run (Figure 5b) similarly to the He blowdown run. The He pressurisation was quicker than the He blowdown, taking less than 10 seconds. This was because the gas velocity decreased more quickly in the pressurisation run than in the blowdown run.

The stark difference of the pressurisation dynamics between CO_2 and He can also be explained by the associated gas velocity profiles (Figure 5c). The huge amount of CO_2 is needed to pressurise the column due to most of the CO_2 supplied to the column

being used for adsorption rather than for pressurisation, while the relatively small amount of He is sufficient to fill in the column up to the same pressure. The huge difference of the amount of gas required for pressurisation between CO_2 and He led to the CO_2 velocity at the column inlet being much greater than the He velocity (Figure 5c).

The pressure inside the column affects greatly the actual gas velocity, so its effect must be taken into account in estimating the actual gas velocity in particular during the pressure-changing steps. For the initial stage of pressurisation when the column pressure is low, the gas entering the column is to be expanded, flowing along the column at a very high velocity. The high gas flowrate would aggravate the pressure drop along the column. But with the column pressure increasing with time during pressurisation, the pressure change direction led to the gas velocity decreasing quickly, resulting in a lesser pressure drop and helping the column pressure reach the target quickly.

The CO_2 and He pressurisation investigated in this study are regarded as two limiting cases. Light product pressurisation would be similar to the He pressurisation, while feed pressurisation would behave somewhere between the two limiting cases depending on the CO_2 mole fraction in the feed and the initial amount of CO_2 remaining inside the column.

4.3. Effect of column length on adsorption dynamics during pressure-varying steps

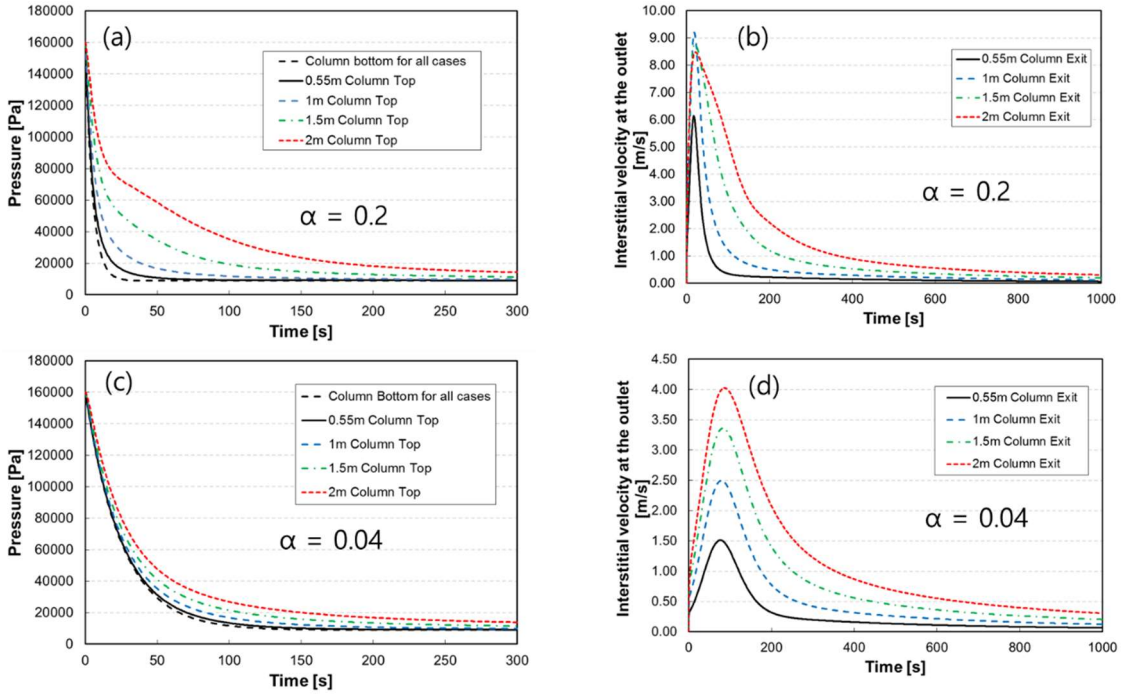

Figure 6. Effects of column length on the pressure and gas velocity profiles in the blowdown simulation of a column saturated with CO_2 in case of fast (α = 0.2) or moderate (α = 0.04) pressure change.

Most of the past researches on CO_2 capture by a 13X VSA have proposed a variety of adsorption processes in which the step configurations and step times were found based on the outcomes of their researches at lab scales (0.2 – 1 m of the column length). However, they have paid less attention to implications of its scale-up to a commercial size. It was alluded to that the step configurations and step times found from the small-scale experiments or their simulations would also be applicable to their large-scale processes without having to make any modification. If the CO_2 capture VSA is to be scaled up to a commercial unit, it is very likely that the adsorption column be greater than 1 m in length [20]. The pressure drop effect must grow greater with the column length increasing, resulting in the pressure-varying step taking much longer that what was estimated in the lab-scale simulation or experiment.

The effect of column length on the pressure drop was investigated by simulation. The pressure change at the column end where gas is admitted to or discharged from was described by Eq. 13. In this study, three scenarios of pressure change at the column boundary were proposed to see the effect of pressure change speed on the column dynamics: fast ($\alpha = 0.2$), moderate ($\alpha = 0.04$) and slow ($\alpha = 0.015$) pressure changes at the bottom end. According to Eq. 13, the pressure at the column end where the gas is admitted to or discharged from reaches 99% of the target pressure after 24, 116 and 308 seconds in the fast, moderate and slow pressure change cases, respectively.

Figure 6 shows the simulation results of depressurising a column initially saturated with pure CO_2 at 1.6 bar to 0.1 bar by pulling a vacuum at the fast or moderate rates. As can be seen clearly in Figure 6a and c, the column would undergo greater pressure drops in the fast rate case than in the moderate rate case. It should be noted that the depressurisation could be completed more quickly by forcing the pressure on one column end to decrease faster. But such improvement caused by a faster pressure change would be feasible only if the column was relatively short, e.g. 0.55 m long column (see Figure 6a and c). With increasing column length, the time taken for depressurisation becomes longer. And the effect of column length on the required depressurisation time is more salient in the fast rate case (Figure 6a) than in the moderate rate case (Figure 6c). In the end, the two depressurisation times in the fast and moderate rate cases are similar to each other for the 2 m long column. The pressure drop estimated by simulation (Figure 6a and c) matches well the gas velocity profiles at the column exit as shown in Figure 6b and d.

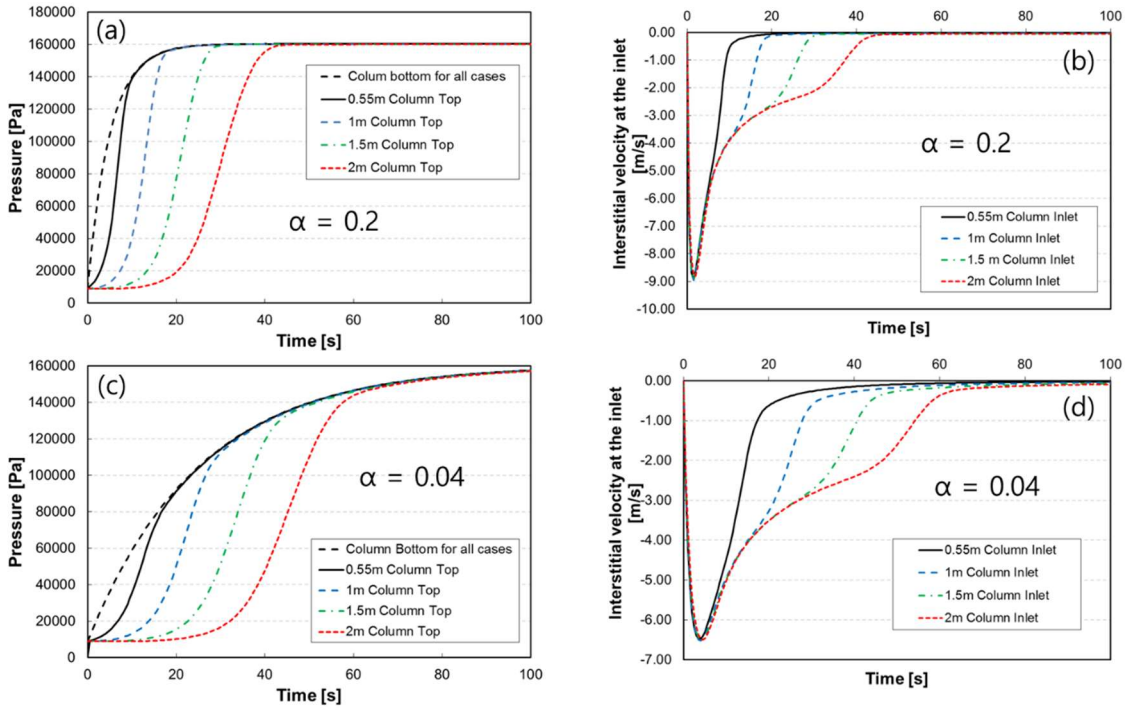

Figure 7. Effects of column lengths on the pressure drop and gas velocity profiles in the CO_2 pressurisation simulation in case of fast (α = 0.2) or moderate (α = 0.04) pressure change.

A parametric study was also carried out for pressurisation of the evacuated column at 0.1 bar with pure CO_2 up to 1.6 bar. Similarly to the blowdown parametric study, the pressurisation simulations were performed with the column length ranging 0.55 to 2 m, for three scenarios of the pressure change on the bottom end: high, moderate and low rate cases. The simulation results of the high and moderate rate cases are presented in Figure 7. As expected, the pressure drop becomes larger with increasing column length. However, the column dynamics of pressurisation is very different from those of blowdown, as they show a very large pressure drop soon after the onset but the pressure drop disappears quickly thereafter. As shown in Figure 7a and c, all the lines for different column lengths converge to the pressure profile imposed on the column end, before the column end pressure reaches the target, indicating that the times taken for pressurisation would be similar, regardless of the column length. In other words, the time taken for pressurisation is mainly dependent on the pressure change rate on one

column end, hardly affected by the column length. On the contrary, the blowdown time is strongly affected by the column length and attempting to shorten the blowdown time by making the pressure change at one column end faster would be effective only for a short column.

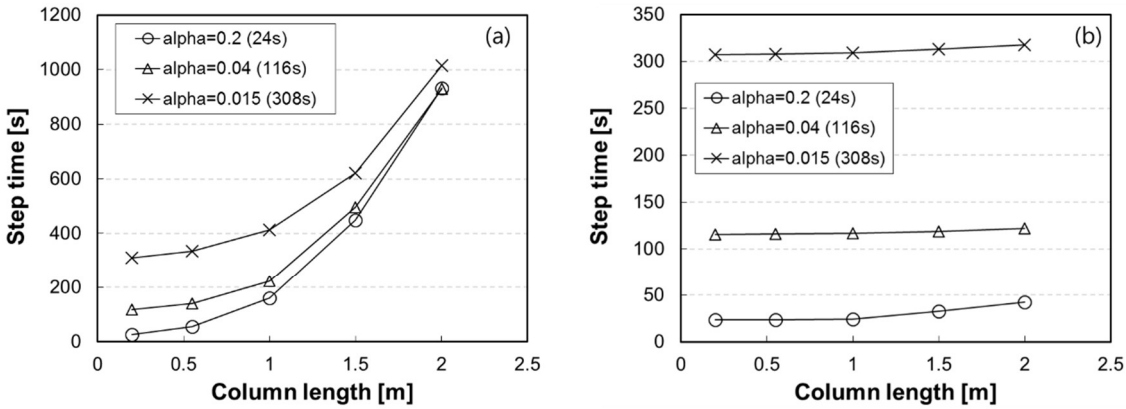

Figure 8. Effect of column length on times taken to reach 99% of the target pressure during (a) blowdown of a CO_2 saturated column and (b) pressurization of an evacuated column with CO_2: The numbers in the parenthesis indicate the times taken for the pressure at one column end where the gas is admitted to or discharged from to reach the target pressure.

In Figure 8, the simulation results of the parametric studies were rearranged to show clearly the effect of column length on the time taken to reach the target pressure during the pressure-varying steps. As discussed above, the required blowdown time increases rapidly with the column length, while the pressurisation time is rarely affected by the column length. For the 2 m long column, the blowdown would take as long as 900 seconds, however fast the pressure change was made on one column end. In stark contrast to the blowdown, the pressurisation of the long column could be completed much more quickly, less than 50 seconds, as long as the pressure was changed fast on the bottom end (α=0.2).

In designing a CO_2 capture VSA unit, it is critical to have the cycle time as short as possible for enhancing the bed productivity. To this end, it is recommended to make the step configuration contain as few idle steps as possible and minimise the step times

assigned for blowdown and pressurisation as well as constant-pressure steps. In this respect, the blowdown and pressurisation step times must be chosen so as not to have each step last longer than the time needed for the pressure change.

As a result of the parametric study, several guidelines are concluded as to how to assign the pressure-varying step times of a CO_2 capture 13X VSA, in particular with more attention paid to the case that the column length has to be long enough for its commercial application.

- The longer the column becomes, the more time has to be assigned to the BD step. At a short column, the required BD time could be shortened by making faster the pressure change at one column end. However, the effect of having the pressure change faster on the BD time wears off gradually with increasing column length. In the end, the required BD times are almost identical for 2 m long column, regardless of the pressure change rate at one column end. In other words, there is no need to make faster the pressure change rate at one column end during BD in case of such a long column (Figure 8a).
- As for PR step, the required time could be made shorter by making faster the pressure change at one column end, hardly affected by the column length (Figure 8b).
- It is possible to reduce the PR time further by supplying the feed gas at a pressure much higher than the target adsorption pressure. On the contrary, reducing the BD time would be harder due to the achievable vacuum pressure being often very limited. Feeding the gas of an excessive pressure into the column is capable of making the pressure change faster, but the adsorption column often undergoes a pressure overshoot (see Figures 2a and 5a). After

reaching a pressure over the target, the column pressure returns gradually to the set value by releasing the gas to the outside through the back pressure regulator. The pressure overshoot would occur when the back pressure regulator was unable to respond to the pressure change quickly enough to control the column pressure below the target.

- Apart from the column length, the pressure drop during the pressure-varying steps and the resulting time required for the step are affected by many other factors, such as bead shape/size, bed void fraction that often depends on how well the bed is packed (dense or loose), adsorption capacity/rate, gas composition, etc. The column dynamics must be evaluated in the course of a VSA process design in order to estimate the times required for pressure-varying steps, and they can be predicted reasonably well by numerical simulation.

4.4. Implications of scale-up on step configuration and column design

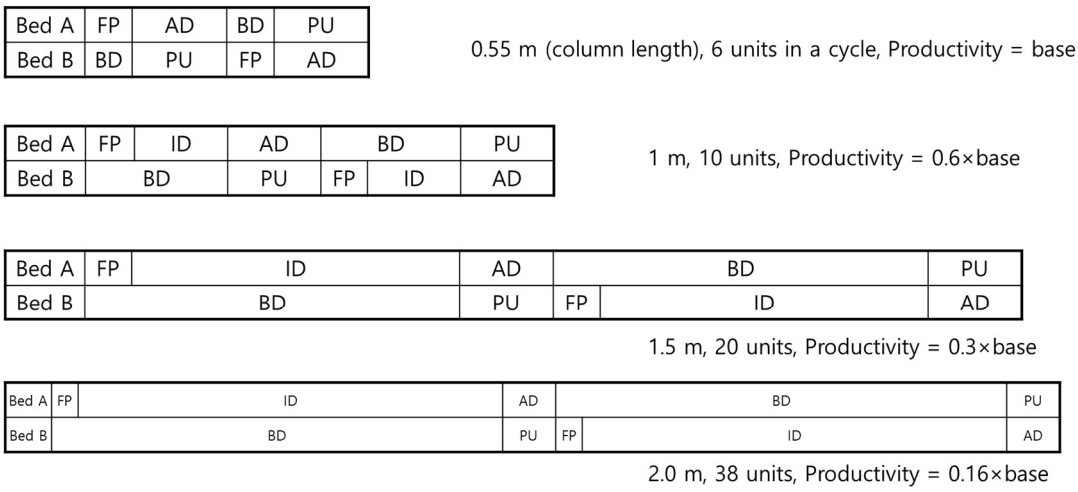

Figure 9. Examples of the step configuration of a CO_2 capture 13X VSA cycle with the column length changing from 0.55 m to 2.0 m in case of α = 0.2 (FP: Feed Pressurisation, AD: Adsorption, BD: Blowdown, PU: product purge, ID: idle).

Based upon the required step times presented in Figure 8, step configurations of a CO_2 capture 13X VSA cycle were proposed under the condition of the fast pressure change

on one column end, i.e. α=0.2 (Figure 9). At the column length of 0.55 m, the two pressure-varying step times could be equal to each other due to negligible pressure drop effect. It was assumed that the AD (or PU) step times would be equal to each other, double the FP step time. The bed productivity of the CO_2 capture VSA consisting of two 0.55 m long columns was considered as the base case. At 1m, the required BD time is around 161 seconds, triple the FP time. Likewise, the required BD times for 1.5 and 2.0 m column are nine and seventeen times longer than the FP time. Accordingly, the bed productivity would decrease fast with increasing column length, as the time taken to produce the same amount of CO_2 got longer. The adsorption cycle would indubitably become so inefficient, accommodating a very long idle step to reconcile between the very long BD time and the short FP time, that the 2m long column VSA has as low a bed productivity as only 16% of the 0.55 m long column VSA's productivity.

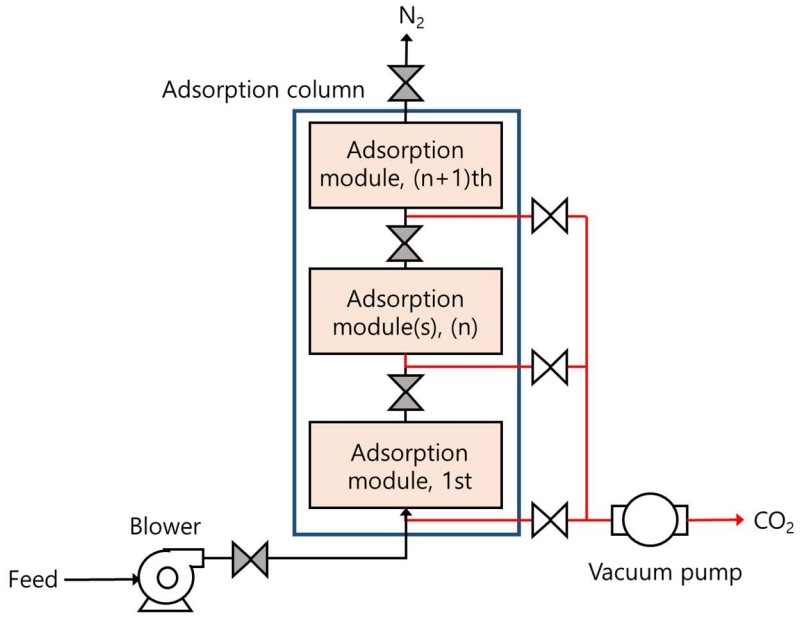

Figure 10. Conceptual design of an adsorption column consisting of low-height, packed-bed adsorption modules for good bed productivity.

The disparity issue of the two pressure-varying step times may be circumvented to some extent by packing the column with adsorbent beads of a larger size to increase the bed void fraction and mitigate the pressure drop. However, there must be an upper limit as to the particle size from the practicality point of view, and also increasing the particle size may result in making the VSA perform worse in the CO_2/13X system in which the adsorption rate is controlled by macropore diffusion. Making use of larger beads may result in the CO_2 adsorption taking more time in reaching the adsorption equilibrium, causing the system to deviate more from its intended equilibrium-driven separation. The larger size the CO_2/13X VSA system is to be scaled up to, the harder it becomes to mitigate the pressure drop issue by increasing the particle size.

However, the pressure drop issue can be resolved by introducing a new column design concept, without having to increase the bead size. Figure 10 depicts a conceptual design of the new column design enabling to avoid a significant pressure drop during the blowdown step, so that the blowdown step time can be similar to the pressurisation step time all the time. It is proposed to have multiple, low-height, packed-beds connected in series with a set of valve and pipe placed between the adsorption modules to isolate and evacuate each module individually during blowdown, while the valves connecting the modules are always open in the other steps. The height of an adsorption module must be chosen carefully based on the performance data, e.g. Figure 8, so that the blowdown and pressurisation step times can be as close to each other as possible. With the structure of vertical stacking rather than spreading modules on the ground, the footprint required for the column could be minimised. All in all, an efficient step configuration of a cycle put forward based on a lab-scale unit still can be applied to its commercial-size unit without any compromise on the process performance but additional space needed for sets of valve and pipe between the

modules. The commercial VSA process can have as high a productivity as what is achievable by the lab-scale equivalent.

5. Conclusions

This study elucidated the column dynamics of a CO_2 capture 13X VSA during the pressure-varying steps in which the actual gas velocity could be faster than those in the constant-pressure steps. By both experiments and simulation, it turns out that the blowdown time has to be extended substantially with increasing column length due to the pressure drop lingering for long, while the pressurisation time would be rarely affected by the length. Accordingly, it is hard to configure an adsorption cycle of a commercial-scale VSA unit in which the blowdown step has to be much longer than the pressurisation step. Inevitably, the bed productivity of the large-scale VSA would be compromised greatly, due to the cycle time having to be extended long enough to accommodate such a long blowdown time. To overcome the step time disparity issue going worse with the unit scaled up to a larger length, a new column design in which low-height, packed-bed adsorption modules are to be stacked vertically has been proposed so as to avoid a large pressure drop during the blowdown step. The alternative column design technology paved the way for enabling a CO_2 capture 13X VSA of any scale to achieve as high a productivity as its lab-scale unit.

Nomenclature

b_i, f_i	Dual-site Langmuir isotherm parameter of component i, Eqs. 10 and 11 (m^3/mol)
$b_{i,0}$, $f_{i,0}$	Arrhenius equation constant, Eqs. 10 and 11 (m^3/mol)
c_i	Gas concentration of component i (mol/m^3)
c_T	Total concentration (mol/m^3)
$\hat{C}_{pa}$	Specific adsorbed phase heat capacity (J/kg/K)
$\hat{C}_{vg}$	Specific gas heat capacity (J/kg/K)
$\hat{C}_{ps}$	Specific adsorbent heat capacity (J/kg/K)
$\hat{C}_{pw}$	Specific wall heat capacity (J/kg/K)
D_g	Diffusivity in the gas phase (m^2/s)
D_K	Knudsen diffusivity (m^2/s)
D_p	Pore diffusivity (m^2/s)
D_z	Axial dispersion coefficient (m^2/s)
d_p	Adsorbent diameter (m)
D_v	Viscous diffusivity (m^2/s)
F_v	Gas volumetric flowrate, Eq. 15 (m^3/s)
$-\Delta H_i$	heat of adsorption of component i (J/mol)
h_{in}	Heat transfer coefficient at the inner wall (W/m^2/K)
h_{out}	Heat transfer coefficient at the outer wall (W/m^2/K)
k_{LDF}	LDF parameter (1/s)
k_z	Axial thermal dispersion (W/m/K)
M	Molecular weight (mol/kg)
n	Number of components (-)
P	Pressure (kPa)
P_H	Target (or initial) pressure of pressurisation (or blowdown) (kPa)
P_L	Target (or initial) pressure of blowdown (or pressurisation) (kPa)
ΔP	Pressure change through the filter, Eq.15 [bar]
Pr	Prandtl number (-)
q_i^*	Adsorbed amount of component i in equilibrium with its gas phase concentration (mol/kg)
$\bar{q}_i$	Adsorbed amount of component i (mol/kg)
q_i^{eq}	Adsorbed amount of component i at equilibrium, Eq. 10 (mol/kg)
$q_{sb,i}$, $q_{sf,i}$	Saturated adsorbed amount of component i, Eq. 10 (mol/kg)
r	Average radius of macropores (m)
R	Universal gas constant (kPa·m^3/mol/K)
Re	Reynolds number (-)
Sc	Schmidt number (-)
T	Temperature (K)
T_a	Ambient temperature (K)
t	time (s)
u	Interstitial gas velocity (m/s)
$-\Delta U_{b,I}$ $-\Delta U_{f,i}$	Arrhenius equation parameter, Eq. 10 (J/mol)
y_i	Gas mole fraction of component i (-)
z	Axial direction (m)

Greek Letters	
α	Coefficient of Eqs.13 and 14 indicating how fast the pressure changes at one column end during pressure-varying steps (-)
ε	Interparticle void fraction in the bed (-)
ε_p	Macropore void fraction in the pellet (-)
μ	Viscosity (Pa·s)
ρ_s	Adsorbent density (kg/m^3)
ρ_g	Gas density (kg/m^3)
ρ_{ads}	Adsorbed phase density (kg/m^3)
ρ_w	Column wall density (kg/m^3)
τ	Tortuosity (-)
Subscripts	
i	Component i

Abbreviation	
AD	Adsorption/Feed
BD	Blowdown
BECCS	Bio-Energy Carbon Capture and Storage
CCC	The Committee on Climate Change
CCS	Carbon Capture and Storage
LDF	Linear Driving Force
PR	Pressurisation
PU	Purge
VSA	Vacuum Swing Adsorption

Acknowledgements

Dr Ahn had carried out part of this work while on his sabbatical leave in Yonsei University as a Brain Pool Fellow funded by the Korean Federation of Science and Technology Societies (KOFST) grant (No. 172S-5-3-1977). The financial support from British Embassy Seoul through the UK-Korea Focal Point Programme is also greatly appreciated.

References

1. Net Zero: The UK's Contribution to Stopping Global Warming. In Committe on Climate Change: 2019.

2. *Carbon Capture Usage and Storage: Third Time Luckly?*; Business, Energy and Industrial Strategy Committee: UK, 2019.

3. Rubin, E. S.; Davison, J. E.; Herzog, H. J., The Cost of CO2 Capture and Storage. *International Journal of Greenhouse Gas Control* **2015,** 40, 378 - 400.

4. Ahn, H.; Luberti, M.; Liu, Z.; Brandani, S., Process Configuration Studies of the Amine Capture Process for Coal-Fired Power Plants. *International Journal of Greenhouse Gas Control*

2013, 16, 29 - 40.

5. *Techno-Economic Evaluation of SMR Based Standalone (Merchant) Hydrogen Plant with CCS*; UK.

6. Bui, M.; Adjiman, C. S.; Bardow, A.; Anthony, E. J.; Boston, A.; Brown, S.; al., e., Carbon Capture and Storage (CCS): the Way Forward. *Energy & Environmental Science* **2018,** 11, 1062 - 1176.

7. Oreggioni, G. D.; Brandani, S.; Luberti, M.; Baykan, Y.; Friedrich, D.; Ahn, H., CO2 Capture from Syngas by an Adsorption Process at a Biomass Gasification CHP Plant: Its Comparison with Amine-Based CO2 Capture. *International Journal of Greenhouse Gas Control* **2015,** 35, 71 - 81.

8. Ruthven, D. M., *Principles of Adsorption and Adsorption Processes*. John Wiley & Sons, Inc.: 1984.

9. Ruthven, D. M.; Farooq, S.; Knaebel, K. S., *Pressure Swing Adsorption*. Wiley-VCH: 1993.

10. Chue, K. T.; Kim, J. N.; Yoo, Y. J.; Cho, S. H.; Yang, R. T., Comparison of Activated Carbon and Zeolite 13X for CO2 Recovery from Flue Gas by Pressure Swing Adsorption. *Ind. Eng. Chem. Res.* **1995,** 34, 591 - 598.

11. Ko, D.; Siriwardane, R.; Biegler, L. T., Optimisation of Pressure Swing Adsorption and Fractionated Vacuum Pressure Swing Adsorption Processes for CO2 Capture. *Ind. Eng. Chem. Res.* **2005,** 44, 8084 - 8094.

12. Xiao, P.; Zhang, J.; Webley, P.; Gang, L.; Singh, R.; Todd, R., Capture of CO2 from Flue Gas Streams with Zeolite 13X by Vacuum-Pressure Swing Adsorption. *Adsorption* **2008,** 14, 575 - 582.

13. Haghpanah, R.; Majumder, A.; Nilam, R.; Rajendran, A.; Farooq, S.; Karimi, I. A.; Amanullah, M., Multiobjective Optimization of a Four-Step Adsorption Process for Postcombustion CO2 Capture Via Finite Volume Simulation. *Ind. Eng. Chem. Res.* **2013,** 52, 4249 - 4265.

14. Li, G.; Xiao, P.; Webley, P.; Zhang, J.; Singh, R.; Marshall, M., Capture of CO2 from High Humidity Flue Gas by Vacuum Swing Adsorption with Zeolite 13X. *Adsorption* **2008,** 14, 415 - 422.

15. Hasan, M. M. F.; Baliban, R. C.; Eila, J. A.; Floudas, C. A., Modeling, Simulation, and Optimization of Postcombustion CO2 Capture for Variable Feed Concentration and Flow Rate. 2. Pressure Swing Adsorption and Vacuum Swing Adsorption Processes. *Ind. Eng. Chem. Res.* **2012,** 51, 15665 - 15682.

16. Krishnamurthy, S.; Rao, V. R.; Guntuka, S.; Sharratt, P.; Haghpanah, R.; Rajendran, A.; Amanullah, M.; Karimi, I. A.; Farooq, S., CO2 Capture from Dry Flue Gas by Vacuum Swing Adsorption: A Pilot Plant Study. *AIChE Journal* **2014,** 60, (5), 1830 - 1842.

17. Ling, J.; Ntiamoah, A.; Xiao, P.; Webley, P. A.; Zhai, Y., Effects of Feed Gas Concentration,

Temperature and Process Parameters on Vacuum Swing Adsorption Performance for CO2 Capture. *Chemical Engineering Journal* **2015,** 265, 47 - 57.

18. Luberti, M.; Oreggioni, G. D.; Ahn, H., Design of a Rapid Vacuum Pressure Swing Adsorption (RVPSA) Process for Post-Combustion CO_2 Capture from a Biomass-fuelled CHP Plant. *Journal of Environmental Chemical Engineering* **2017,** 5, (4), 3973 - 3982.

19. Ntiamoah, A.; Ling, J.; Xiao, P.; Webley, P. A.; Zhai, Y., CO2 Capture by Vacuum Swing Adsorption: Role of Multiple Pressure Equalization Steps. *Adsorption* **2015,** 21, 509 - 522.

20. Susarla, N.; Haghpanah, R.; Karimi, I. A.; Farooq, S.; Rajendran, A.; Tan, L. S. C.; Lim, J. S. T., Energy and Cost Estimates for Capturing CO2 from a Dry Flue Gas Using Pressure/Vacuum Swing Adsorption. *Chemical Engineering Research and Design* **2015,** 102, 354 - 367.

21. Zhao, R.; Deng, S.; Zhao, L.; Zhao, Y.; Li, S.; Zhang, Y.; Yu, Z., Experimental Study and Energy-Efficiency Evaluation of a 4-step Pressure-Vacuum Swing Adsorption (PVSA) for CO2 Capture. *Energy Conversion and Management* **2017,** 151, 179 - 189.

22. Haghpanah, R.; Nilam, R.; Rajendran, A.; Farooq, S.; Karimi, I. A., Cycle Synthesis and Optimization of a VSA Process for Postcombustion CO2 Capture. *AIChE Journal* **2013,** 59, 4735 - 4748.

23. Leperi, K. T.; Snurr, R. Q.; You, F., Optimization of Two-Stage Pressure/Vacuum Swing Adsorption with Variable Dehydration Level for Postcombustion Carbon Capture. *Ind. Eng. Chem. Res.* **2016,** 55, (3338 - 3350).

24. Hu, X.; Mangano, E.; Friedrich, D.; Ahn, H.; Brandani, S., Diffusion Mechanism of CO2 in 13X Zeolite Beads. *Adsorption* **2014,** 20, (1), 121 - 135.

25. Liu, Z.; Grande, C. A.; Li, P.; Yu, J.; Rodrigues, A. E., Multi-bed Vacuum Pressure Swing Adsorption for Carbon Dioxide Capture from Flue Gas. *Separation and Purification Technology* **2011,** 81, 307 - 317.

26. Luberti, M.; Kim, Y.-H.; Lee, C.-H.; Ferrari, M.-C.; Ahn, H., New Momentum and Energy Balance Equations Considering Kinetic Energy Effect for Mathematical Modelling of a Fixed-bed Adsorption Column. *Adsorption* **2015,** 21, (5), 353 - 363.

27. Wang, Y.; LeVan, M. D., Adsorption Equilibrium of Binary Mixtures of Carbon Dioxide and Water Vapor on Zeolites 5A and 13X. *Journal of Chemical & Engineering Data* **2010,** 55, 3189 - 3195.

28. Wakao, N.; Funazkri, T., Effect of Fluid Dispersion Coefficients on Particle-to-fluid Mass Transfer Coefficients in Packed Beds. *Chemical Engineering Science* **1978,** 33, 1375 - 1384.

29. Kim, J.-J.; Lim, S.-J.; Ahn, H.; Lee, C.-H., Adsorption Equilibria and Kinetics of Propane and Propylene on Zeolite 13X Pellets. *Microporous and Mesoporous Materials* **2019,** 274, 286 - 298.

30. Park, Y.; Ju, Y.; Park, D.; Lee, C.-H., Adsorption Equilbria and Kinetics of Six Pure Gases on Pelletized Zeolite 13X up to 1.0 MPa: CO2, CO, N2, CH4, Ar and H2. *Chemical Engineering*

Journal **2016,** 292, 348 - 365.

31. Swagelok, Filters - FW, F, and TF Series, MS-01092, RevL. In 2017.